Vicariance and dispersal events inferred from mitochondrial genomes and nuclear genes (*18S*, *28S*) shaped global *Cryptocercus* distributions

Yanli Che [a], Wenbo Deng [a], Weijun Li [a], Jiawei Zhang [a], Yukihiro Kinjo [c], Gaku Tokuda [d], Thomas Bourguignon [c,e], Nathan Lo [b,*], Zongqing Wang [a,*]

[a] *College of Plant Protection, Southwest University, Beibei, Chongqing 400716, PR China*
[b] *School of Life and Environmental Sciences, University of Sydney, Sydney, NSW 2006, Australia*
[c] *Okinawa Institute of Science & Technology Graduate University, 1919–1 Tancha, Onna-son, Okinawa 904–0495, Japan*
[d] *Tropical Biosphere Research Center, Center of Molecular Biosciences, University of the Ryukyus, Nishihara, Okinawa 903-0213, Japan*
[e] *Faculty of Tropical AgriSciences, Czech University of Life Sciences, Kamycka 129, Prague CZ-165 00, Czech Republic*

ARTICLE INFO

ABSTRACT

Cryptocercus Scudder, a genus of wingless, subsocial cockroaches, has low vagility but exhibits a disjunct distribution in eastern and western North America, and in China, South Korea and the Russian Far East. This distribution provides an ideal model for testing hypotheses of vicariance through plate tectonics or other natural barriers versus dispersal across oceans or other natural barriers. We sequenced 45 samples of *Cryptocercus* to resolve phylogenetic relationships among members of the genus worldwide. We identified four types of tRNA rearrangements among samples from the Qin-Daba Mountains. Our maximum-likelihood and Bayesian phylogenetic trees, based on mitochondrial genomes and nuclear genes (*18S*, *28S*), strongly supported six major lineages of *Cryptocercus*, which displayed a clear geographical distribution pattern. We used Bayesian molecular dating to estimate the evolutionary timescale of the genus, and reconstructed *Cryptocercus* ancestral ranges using statistical dispersal-vicariance analysis (S-DIVA) in RASP. Two dispersal events and six vicariance events for *Cryptocercus* were inferred with high support. The initial vicariance event occurred between American and Asian lineages at 80.5 Ma (95% credibility interval: 60.0–104.7 Ma), followed by one vicariance event within the American lineage 43.8 Ma (95% CI: 32.0–57.5 Ma), and two dispersal 31.9 Ma (95% CI: 25.8–39.5 Ma), 21.7 Ma (95% CI: 17.3–27.1 Ma) plus four vicariance events *c.* 29.3 Ma, 27.2 Ma, 24.8 Ma and 16.7 Ma within the Asian lineage. Our analyses provide evidence that both vicariance and dispersal have played important roles in shaping the distribution and diversity of these woodroaches.

1. Introduction

The subsocial cockroach genus *Cryptocercus* and the eusocial termites descend from a common ancestor that existed in the late Jurassic to early Cretaceous (Che et al., 2016, 2020; Misof et al., 2014), prior to the beginning of breakup of Laurasia. *Cryptocercus* is a wingless genus with low vagility, exhibiting a disjunct distribution in the northern Hemisphere (Asia and North America) (Fig. 1). It lives in and feeds on dead wood throughout its life (Maekawa and Nalepa, 2011). It is the continuous availability of rotten logs that enables *Cryptocercus* to survive in sometimes harsh environments (Nalepa et al., 1997). *Cryptocercus* species are typically narrowly distributed and restricted to a limited area (Che et al., 2016, 2020; Wang et al., 2019; Burnside et al., 1999; Nalepa

et al., 1997, 2002), with some exceptions (e.g. *C. relictus* and *C. changbaiensis*, which are widely distributed around the Changbai Mountains, Che et al., 2020). Continental uplifting, glacial extinction events and volcanic orogeny are likely to have shaped the current distributions of *C. relictus* and *C. changbaiensis* (Che et al., 2020). Vicariance events and succession of host plants are believed to have played an important role in the continental distribution of *Cryptocercus* (Nalepa et al. 2002; Che et al. 2020).

The relative importance of vicariance and dispersal events in shaping the current world geographical pattern of insects is a topic of active research (Toussaint and Gillett, 2018; Cui et al., 2015; Barber-James et al., 2008; Krosch and Cranston, 2013; Bourguignon et al., 2016, 2017; Andújar et al., 2012). The global distribution of cockroaches is

---

thought to have been shaped by several vicariance events through plate tectonics, as well as transoceanic dispersal events (Bourguignon et al., 2018). Despite lacking the ability to sustain long-distance flight (Peck and Roth, 1992), most cockroaches have strong short-distance flight capability (Bell et al., 2007). Cockroaches, including wingless and wing-reduced species, are also able to disperse over water through rafting in floating debris and vegetation (Peck, 1990; Peck and Roth, 1992; Trewick, 2001). Because they are wingless and display low dispersal ability, morphological conservatism and disjunct distributions, members of the genus *Cryptocercus* represent an ideal model for testing hypotheses of vicariance and dispersal, and understanding the role of geography in processes of species formation and maintenance of local differentiation.

The insect mitochondrial (mt) genome is a compact circular molecule, including 13 protein-coding genes (PCGs), two rRNA (rRNA) genes 22 tRNA (tRNA) genes, and a variety of non-coding regions. Because of various advantages of mt genome data (e.g. the abundance of mt genomes in tissues, a fast rate of evolution, and conserved transcription products (Cameron, 2014; Crampton-Platt et al., 2016; Simon et al., 2006)), a wide array of studies have used them to infer phylogenetic relationships and resolve questions that have not been answered based on partial mitochondrial sequences or nuclear gene markers (Bourguignon et al., 2016, 2017, 2018; Du et al., 2019; Liu et al., 2019; Song et al., 2019). Recent phylogenetic studies (Che et al., 2016, 2020; Wang et al., 2019) based on partial mitochondrial sequences or nuclear gene markers have improved our knowledge of the relationships among Asian *Cryptocercus* and speciation events in the Hengduan Moutains. However, relationships among some taxa remain unresolved (e.g. whether or not *Cryptocercus* groups in the Hengduan Mountains are paraphyletic).

The arrangement of genes in insect mt genomes is generally thought to be highly conserved for most taxa (Cameron, 2014; McBride et al., 2006), although rearrangements of protein-coding and tRNA genes have been reported in a number of taxa, including barklice (Liu et al., 2017a) and grass thrips (Liu et al., 2017b), and rearrangement of tRNA genes and pseudo genes were also found in assassin bugs (Jiang et al., 2016). The first mitochondrial rearrangement in a representative of the order Blattodea was reported in *C. meridianus* (Li et al., 2017) (occurring between ND3-ND5).

In the present study, we sequenced 45 mitochondrial genomes to complement existing data representing five *Cryptocercus* species, and also obtained nuclear genes (*18S*, *28S*), with the aim of resolving phylogenetic relationships among these taxa. Based on a broad sampling of *Cryptocercus* representatives from both Asia and America, we reconstruct the phylogeny of *Cryptocercus* and examine the evolutionary history of the group through fossil-calibrated divergence dating analysis.

2. Materials and methods

2.1. Taxon sampling, mitochondrial and nuclear genomic DNA extraction, and sequencing

45 samples representing 30 *Cryptocercus* species and one *Cryptocercus* species group were obtained in the field (Table S1), of which, 34 specimens of *Cryptocercus* were collected from Changbai Mountains, Qin-Daba Mountains and Hengduan Mountains in China, and the other 11 samples from California, Tennessee, North Carolina, Virginia and Georgia, USA. All specimens were preserved in 100% ethanol and stored at −80 °C. All voucher specimens are deposited in the Institute of Entomology, College of Plant Protection, Southwest University, Chongqing, China.

Total genomic DNA was extracted from fresh muscle of one leg using the TIANamp Genomic DNA Kit (DP304, TIANGEN, Beijing, China). DNA Libraries were prepared for each sample separately. Forty-five libraries were pooled together and paired-end sequenced in one lane of Illumina HiSeq2500 at Shanghai Genesky Biotechnologies Inc. (China) with 150-bp paired-end reads setting. Raw reads were generated and quality-trimmed with CLC Genomics Workbench v9 (CLC Bio, Aarhus, Denmark). Genome annotation was conducted in Geneious Prime (Biomatters Ltd., Auckland New Zealand) by aligning with those of published *Cryptocercus* mitochondrial genomes. A physical map was drawn with the web based tool OGDRAW (http://ogdraw.mpimp-golm.mpg.
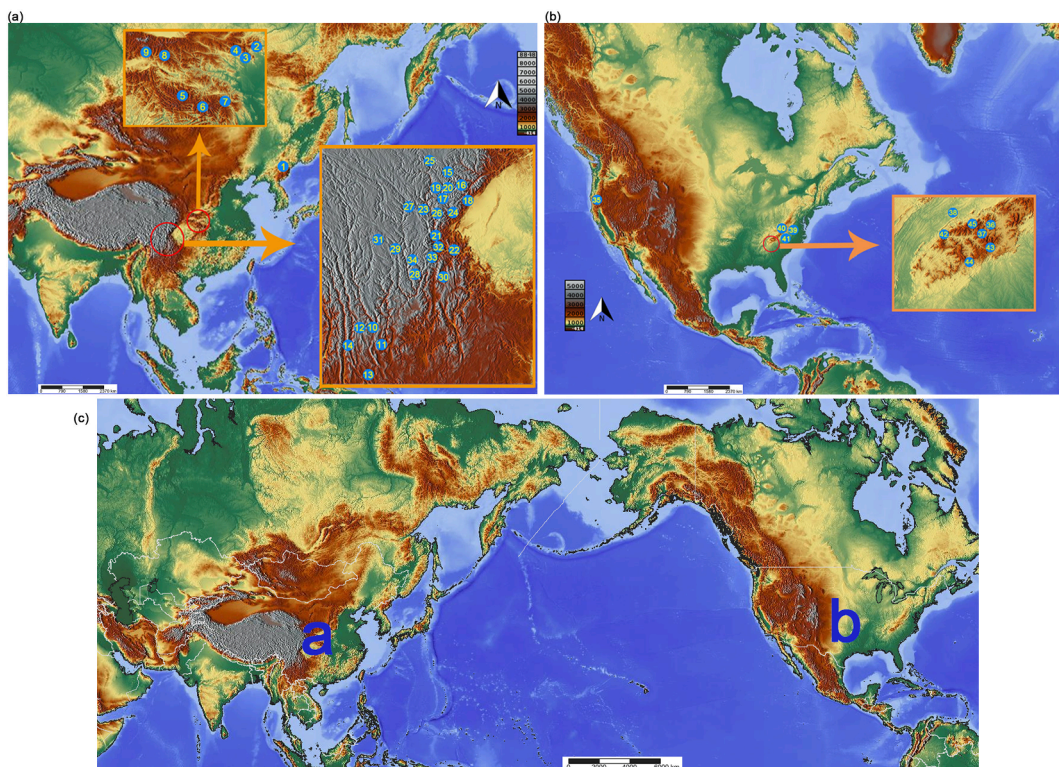

Fig. 1. Sampling locations of *Cryptocercus* cockroaches. Detailed information for these locations is provided in Table S1.

de) (Lohse et al., 2013).

For each mitochondrial contig, annotation of tRNA genes was performed using MITOS webservers (Bernt et al., 2013) with the invertebrate genetic code and default settings and TRNACAN-SE (Lowe and Eddy, 1997). Protein-coding genes (PCGs) and rRNA genes were identified by alignment with homologous genes of previously sequenced *Cryptocercus* mitochondrial genomes. For nuclear 18S rRNA (*18S*) and 28S rRNA (*28S*), the assembling was conducted in Geneious Prime (Biomatters Ltd., Auckland, New Zealand) by aligning with the published *Cryptocercus* data. The annotated mitochondrial genome sequences of 45 *Cryptocercus* specimens, with the length ranging from 14,945 bp to 17,793 bp, and the nuclear 18S rRNA (*18S*) and 28S rRNA (*28S*), with the length 1,932 bp to 1,945 bp, 4,705 bp to 4,875 bp, respectively, have been deposited in GenBank (Table S1).

2.2. Sequence alignment and dataset

To infer the position of the root in our phylogenetic analysis and to allow informative fossil calibrations to be included for molecular dating, we carried out phylogenetic analyses of 34 *Cryptocercus* species, combined with sequences from 2 mantid species, and 32 species of Blattodea from GenBank (Table S1), including 3 Blattidae, 2 Tryonicidae, 2 Lamproblattidae, 10 Blaberidae and 15 termites. Therefore, the final data set included 84 mitochondrial genomes, 64 *18S* and 63 *28S* sequences of 66 species. Sequences were aligned via the online MAFFT 7 server (http://ma.cbrc.jp/alignment/server/) using the Q-INS-i algorithm. Alignments of protein-coding genes were manually performed on amino acid sequences using MEGA 6.0.6 (Tamura et al., 2013). Alignments of the ribosomal sequences (*12S*, *16S*, *18S* and *28S*) were performed using the default parameters on the online GBlocks Web Tool (Castresana, 2000), with ambiguous characters removed by GBlocks.

Five subsets (RNAPCG12) were included: (1) first and second codon positions (PCG12) of all 13 protein-coding genes; (2) 12S rRNA gene; (3) 16S rRNA gene; (4) 18S rRNA gene; and (5) 28S rRNA gene. In addition, we tested an alternative dataset (six subsets) in which the combined tRNA genes were included (RNAPCG12tRNA). In both cases, we excluded the third codon positions of the protein-coding genes because of the high level of mutational saturation. The third codon position (PCG3) ($I_{SS} = 0.540$) was much more saturated than the first and second codon position (PCG12) ($I_{SS} = 0.145$) as revealed by Xia's method implemented in DAMBE 7 (Xia, 2018), and was much closer to the critical value ($I_{SS-C}Sym = 0.805$; based on 32-taxon simulations), indicating that the third codon position is less suitable for analyzing deep divergences in the *Cryptocercus* phylogeny.

2.3. Phylogenetic analyses

PartitionFinder 1.1.1 (Lanfear et al., 2012) was used to select the most appropriate nucleotide substitution model. Best-fitting substitution model for ND1_pos12, ND4_pos12 and ND4L_pos12 was a TIM model with gamma-distributed rate variation across sites and a proportion of invariable sites (TIM + I + G), *18S* TrNef + I + G. The best model for other partitions was a GTR + I + G model.

Phylogenetic analyses were performed on the combined data set using maximum-likelihood and Bayesian inference. Maximum-likelihood analysis was performed using RAxML 7.7.1 (Stamatakis et al., 2008). We used a gamma distribution to model rate heterogeneity across sites. Node support was estimated using 1000 bootstrap replicates. Bayesian analyses were performed using MrBayes 3.2 (Ronquist et al., 2012). We ran two independent sets of Markov chains, each with one cold and three heated chains, for 10^7 generations each. Samples were drawn every 1000 steps, with the first 25% of samples discarded as burn-in. Convergence was assessed with effective sample size (ESS) values ≥ 200 in Tracer 1.6 (Rambaut et al., 2018).

2.4. Divergence dating analysis

We performed divergence-dating analyses of the mitochondrial genome and nuclear data from *Cryptocercus* species and 34 outgroups using BEAST 1.8.4 (Drummond et al., 2012). For each subset of the data, we assigned the best-fitting model of nucleotide substitution selected by PartitionFinder. We compared two tree priors (Yule process and birth-death process) and allowed rates to vary across branches according to an uncorrelated lognormal relaxed clock (Drummond et al., 2006). For this analysis, the molecular clock was calibrated by specifying exponential prior distributions for the ages of seven nodes in the tree, based on termite and other cockroach fossils (Table 1). Two calibration priors, the hard minimum constraint, and the soft maximum bound, correspondingly the upper 97.5% limit of the probability density, were given according to the youngest and oldest time of the fossil, which appropriately shows the uncertainty of the node time (Ho and Phillips, 2009).

The two Bayesian analyses were each run for 50 million steps across four independent Markov chains, with states sampled every 5000 steps. We combined states using Logcombiner in the BEAST package, checked for sufficient sampling and convergence in Tracer 1.6 (Rambaut et al., 2018) to make sure the ESS was greater than 200. A maximum-clade-credibility tree was obtained using TreeAnnotator in the BEAST package. In our analyses, comparison of marginal likelihoods indicated decisive support for the birth-death process over the Yule process. Therefore, we only present the trees inferred using the birth-death tree prior.

2.5. Biogeographic analysis

We reconstructed the evolution of geographic ranges in *Cryptocercus* using a statistical dispersal-vicariance analysis (S-DIVA) implemented in RASP 3.02 (Yu et al., 2015). Six areas of endemism were defined for the biogeographic analyses: (A) Western Sichuan Plateau in Hengduan Mountains; (B) Yunnan Plateau in Hengduan Mountains; (C) Qin-Daba Mountains; (D) Changbai Mountains including eastern Russia and South Korea; (E) west coast of America and (F) east coast of America.

To account for uncertainty in the tree topology, we loaded all of the sampled trees from our BEAST analysis and discarded the first 500 trees. Outgroup taxa were excluded. For S-DIVA analyses, we used the 'Allow Reconstruction' option with a maximum of 100 reconstructions and three random steps, then a maximum of 1000 reconstructions for the final tree. A maximum number of six areas was allowed at each node. Optimal S-DIVA reconstructions were summarized on the pruned maximum-clade-credibility tree from our Bayesian phylogenetic analysis.

3. Results

3.1. Mitochondrial genomic organization of Cryptocercus spp.

We sequenced 45 mitochondrial genomes from representatives of 31 *Cryptocercus* species, and combined these with a further seven genomes available in GenBank and representing five species. Thirty eight of these 52 mitochondrial genomes are complete, with lengths ranging from 14,945 bp to 17,793 bp and an average A + T content of 74.23%. Among the species represented, mitochondrial genomes of *C. habaensis* were found to have the highest A + T content (81.22%), while *C. neixiangensis* displayed the lowest A + T content (72.68%).

Compared with the generally-accepted mitochondrial gene order (GO) of *Drosophila yakuba*, rearrangements of six tRNAs (*trnA*, *trnR*, *trnN*, *trnS1*, *trnE* and *trnF*) between nad3 and nad5 are found in eight samples from the Qin-Daba Mountains (Figs. 2 and 3), which represent four rearrangement types: (i) loss of *trnA* in *C. wuxiensis* (GO1); (ii) translocation of *trnA* in *C. ningshanensis, C. neixiangensis* (BTM) (GO2), and *C. neixiangensis* (MZL) (GO3); (iii) translocation of *trnA* and duplication of *trnE/F* in *C. hirtus* (GO4) and *C. shennongensis* (GO5); and (iv)

Table 1
Fossils used for calibrating the divergence time estimates of major cockroach clades in this study.

Species	Minimum age (Ma)	Calibration group	Soft maximum bound (97.5% probability)	Reference
Amitermes lucidus	13.8	*Amitermes + Orthognathotermes* (1)	70	Krishna and Grimaldi (2009)
Dolichorhinotermes dominicanus	16	*Dolichorhinotermes + Rhinotermes* (2)	100	Schlemmermeyer and Cancello (2000)
Archeorhinotermes rossi	98.2	Neoisoptera + Kalotermitidae(3)	237	Krishna and Grimaldi (2003)
Valditermes brenanae	130.3	termites + *Cryptocercus* (4)	250	Jarzembowski (1981)
Cretaperiplaneta kaonashi	100.5	Blattidae + Tryonicidae (5)	237	Qiu et al. (2020)
Epilampra	41.3	*Epilampra + Galiblatta* (6)	145	Beccaloni (2014)
Gyna obesa	56	*Gyna + Blaptica + Phoetalia* (7)	145	Piton (1940)

*Numbers after calibration groups are labelled for the calibrated nodes in Fig. 5.
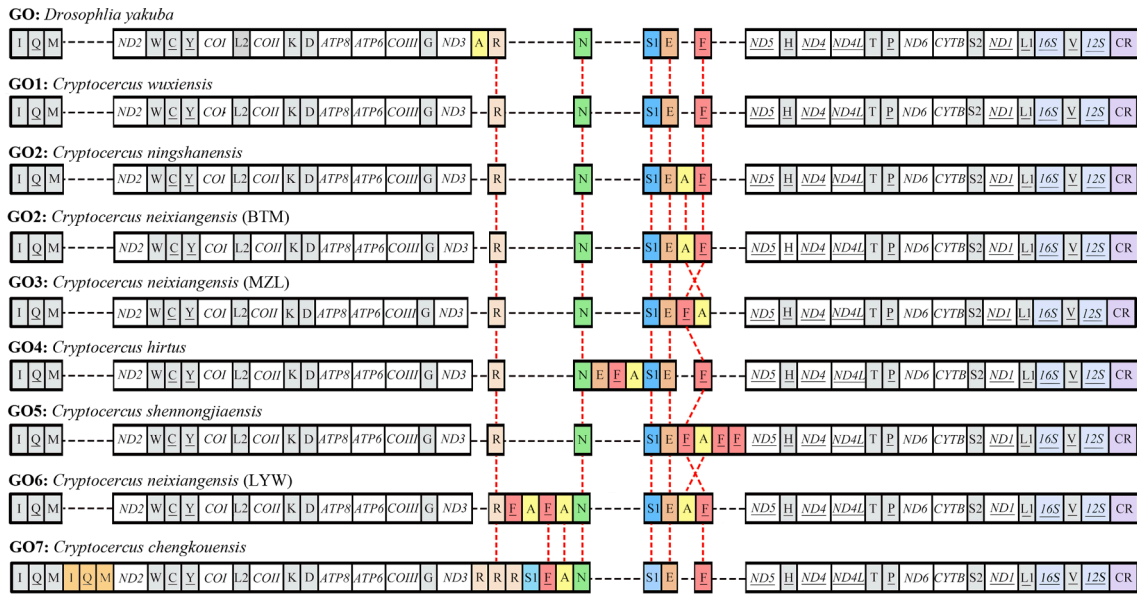

Fig. 2. Mitochondrial gene rearrangements in *Cryptocercus*. Abbreviations of gene names are as follows: *ATP6* and *ATP8*, ATP synthase subunits 6 and 8; *COI-COIII*, cytochrome oxidase subunits 1–3; *CYTB*, cytochrome *b*; *ND1-6* and *ND4L*, NADH dehydrogenase subunits 1–6 and 4L; *16S* and *12S*, large and small rRNA subunits. tRNA genes are indicated by their one-letter corresponding amino acids. CR, control region. Genes are transcribed from left to right except for those that are underlined, which have the opposite transcriptional orientation. Active regions of gene rearrangements were highlighted by color.
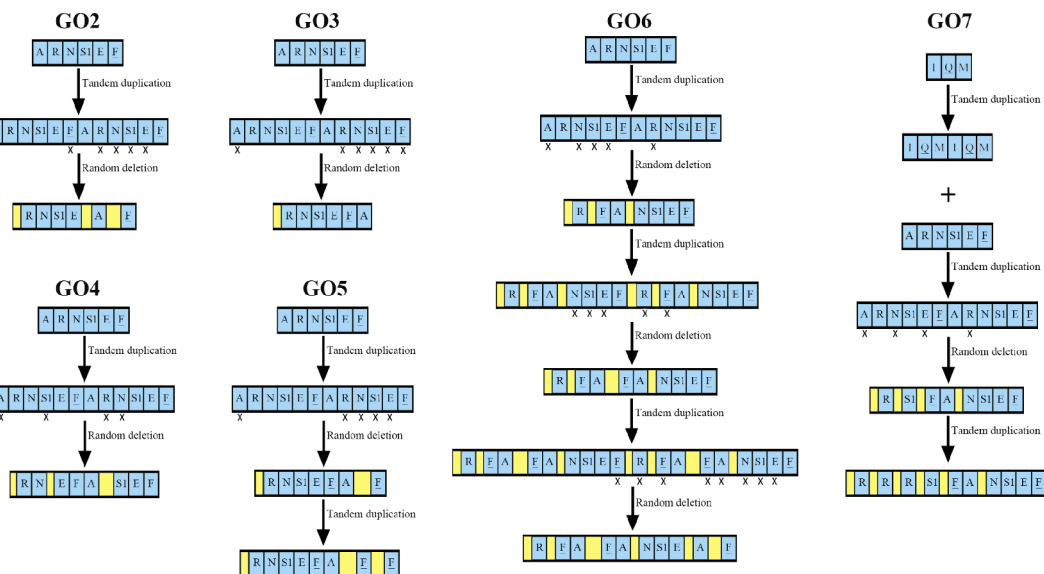

Fig. 3. Inferred TDRL events that account for the mitochondrial gene rearrangements in *Cryptocercus*. (GO2-6) Genes between *ND3* and *ND5*; (GO7) genes between CR and *ND2*, and between *ND3* and *ND5*. Genes with crosses below were eliminated. The longer non-coding sequences are highlighted in yellow. (For interpretation of the references to color in this figure legend, the reader is referred to the web version of this article.)

tandem duplication and random loss in *C. neixiangensis* (LYW) (GO6) and *C. chengkouensis* (GO7). In addition, another rearrangement of three tRNAs (duplication of *trnI-trnQ-trnM*), occurred only in *C. chengkouensis* (GO7).

3.2. Phylogenetic analyses

Phylogenetic analyses were performed using Bayesian inference in MrBayes 3.2 (Ronquist et al., 2012) and using maximum-likelihood in RAxML 7.7.1 (Stamatakis et al., 2008) based on two datasets (RNAPCG12 and RNAPCG12tRNA). Termites and Cryptocercidae were

consistently recovered as sister taxa with strong support values, with a close relationship to the Blattidae + Tryonicidae (Figs. 4, S1-S3).

Based on the RNAPCG12 dataset, both methods yielded highly similar estimates of relationships among *Cryptocercus* spp. (Figs. 4 and S1), with the exception of the position of *C. kagongensis*. We also found strong support for the monophyly of North American *Cryptocercus* and of Asian *Cryptocercus*. In the North American clade, *Cryptocercus clevelandi*, a species from the west coast, was recovered as the sister group of the *C. punctulatus* complex from east coast of America. The samples of *Cryptocercus* from Asia (China, Russia and South Korea) were grouped into four major lineages: clade I from Russia, Northwest China and South
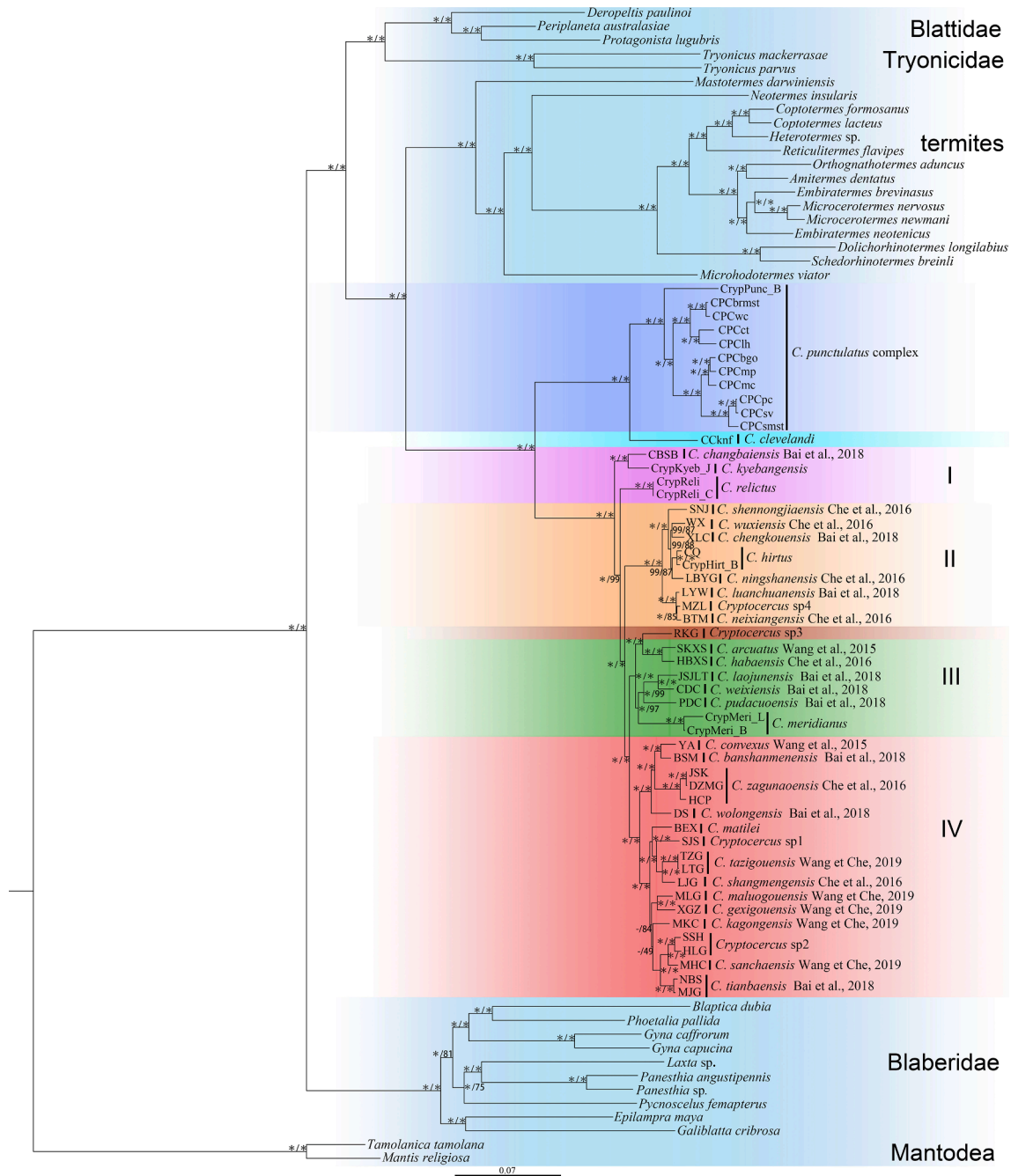

Fig. 4. Bayesian phylogenetic tree inferred from complete mitochondrial genomes (third codon positions and tRNA genes excluded) and nuclear genes (*18S, 28S*). Branches are labelled with Bayesian posterior probabilities (%) and likelihood bootstrap support values. Dashes (−) indicate that the node is absent from the tree inferred in a given analysis; asterisks (*) indicate 100% support. The topology shown is nearly identical to that inferred in our maximum likelihood analysis except MKC. Clade I-IV indicates *Cryptocercus* group from Changbai Mountains including eastern Russia and South Korea, Qin-Daba Mountains, Yunnan Plateau in Hengduan Mountains and Western Sichuan Plateau in Hengduan Mountains, respectively.

Korea; clade II from Qin-Daba Mountains; clade III from the Western Sichuan Plateau in the Hengduan Mountains; and clade IV from the Yunnan Plateau in the Hengduan Mountains with the inclusion of one *Cryptocercus* species from Rekugou, Sichuan Province. Samples of *Cryptocercus* from the Changbai Mountains, including taxa from eastern Russia and South Korea, formed a paraphyletic group. The clade *C. changbaiensis* + *C. kyebangensis* was placed at the basal position as the sister group to the remaining Asian *Cryptocercus*. In both analyses clade III and clade IV were recovered as sister group. This clade plus clade II were recovered as sister group to *C. relictus*. The monophyly of samples of *Cryptocercus* from Hengduan Mountains was strongly supported (ML bootstrap 100%, posterior probability 1), but samples of *Cryptocercus*

from Western Sichuan Plateau were not recovered as monophyletic owing to the *Cryptocercus* species from Rekugou, Sichuan Province.

Based on the RNAPCG12tRNA dataset, our ML and BI phylogenetic analyses produced nearly identical topologies with generally high node support (Figs. S2 and S3), with the exception of the position of *C. ningshanensis* and *C. shennongjiaensis*. In maximum-likelihood analyses that included or excluded the combined tRNA genes, the clade *C. changbaiensis* + *C. kyebangensis* was recovered to be the sister group of the remaining Asian *Cryptocercus* (Figs. 1, S1-S3).
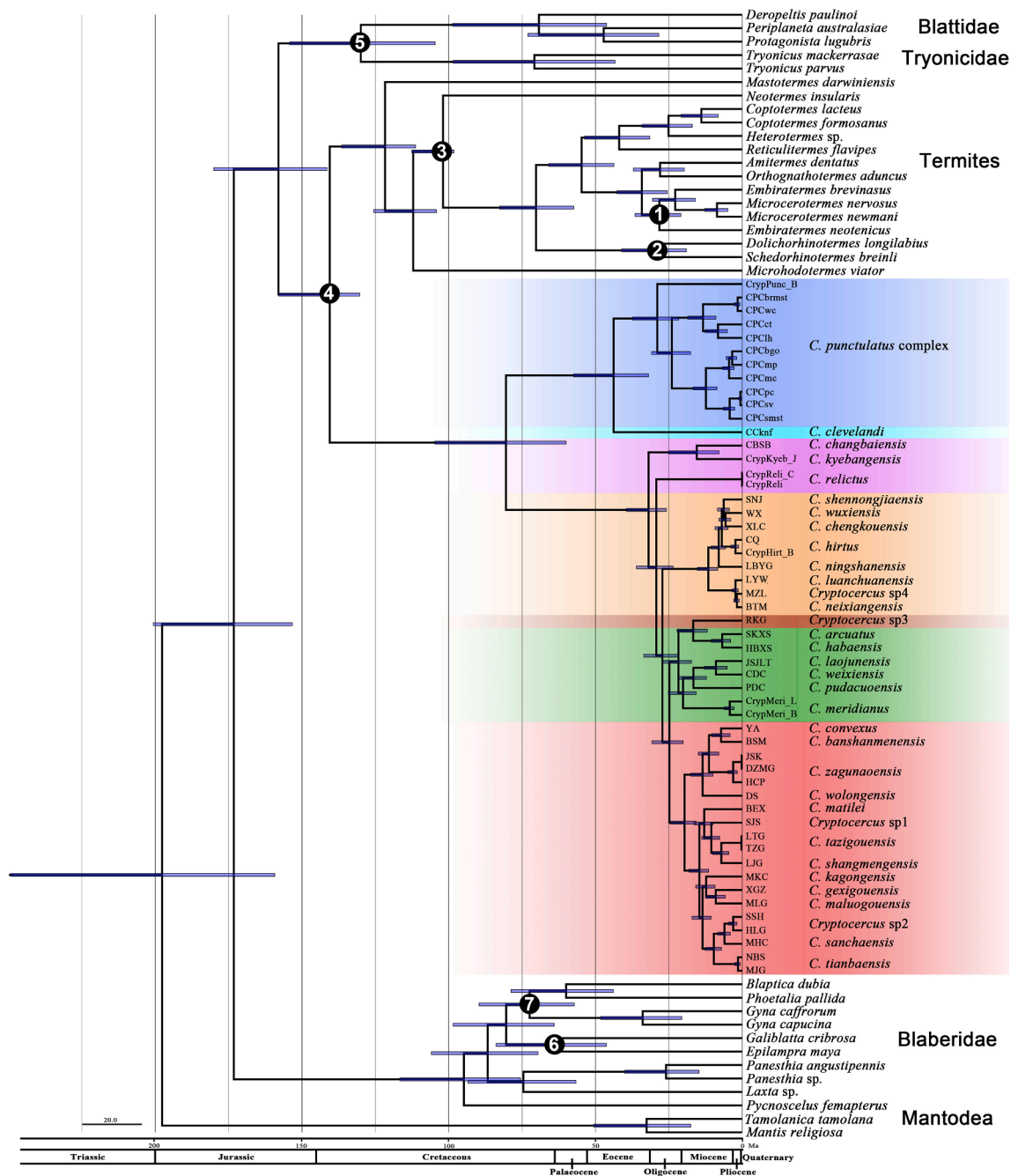

Fig. 5. Chronogram showing *Cryptocercus* phylogeny and divergence time. Consensus tree presenting divergence dates produces by the Beast analysis of the RNAPCG12 dataset using seven fossil calibration points (Numbers 1 – 7 at nodes indicated, more details in Table 1). Blue bars represent 95% credibility intervals for the node ages. A geological time scale is shown at the bottom. (For interpretation of the references to color in this figure legend, the reader is referred to the web version of this article.)

3.3. Divergence dating analysis

The timescale for *Cryptocercus* species diversification based on mitochondrial genomes and nuclear genes (*18S*, *28S*), and calibrated using 7 cockroach (including 3 termites) fossils is shown in Fig. 5 (further details are shown in Table 1). The divergence time analysis indicated that *Cryptocercus* diverged from termites during the Lower Cretaceous to Upper Jurassic, 140.5 Ma (95% credibility interval 130.3–157.9 Ma). Subsequently, *Cryptocercus* diverged into North America *Cryptocercus* and Asian *Cryptocercus c.* 80.5 Ma (95% CI:

60.0–104.7 Ma). In the North American clade, the split between *C. clevelandi* and the *C. punctulatus* complex occurred 43.8 Ma (95% CI: 32.0–57.5 Ma). The *C. punctulatus* complex then diverged 28.9 Ma (95% CI: 21.6–37.4 Ma). Within the *C. punctulatus* complex, the divergence between the two main clades was estimated to date back to 23.9 Ma (95% CI: 17.6–30.9 Ma). In the Asian clade, *C. changbaiensis* + *C. kyebangensis* firstly diverged from other Asian species 31.9 Ma (95% CI: 25.8–39.5 Ma), followed by a divergence between *C. relictus* and the species from the Qin-Daba Mountains and Hengduan Mountains 29.3 Ma (95% CI: 23.6–36.1 Ma). The most recent common ancestor of
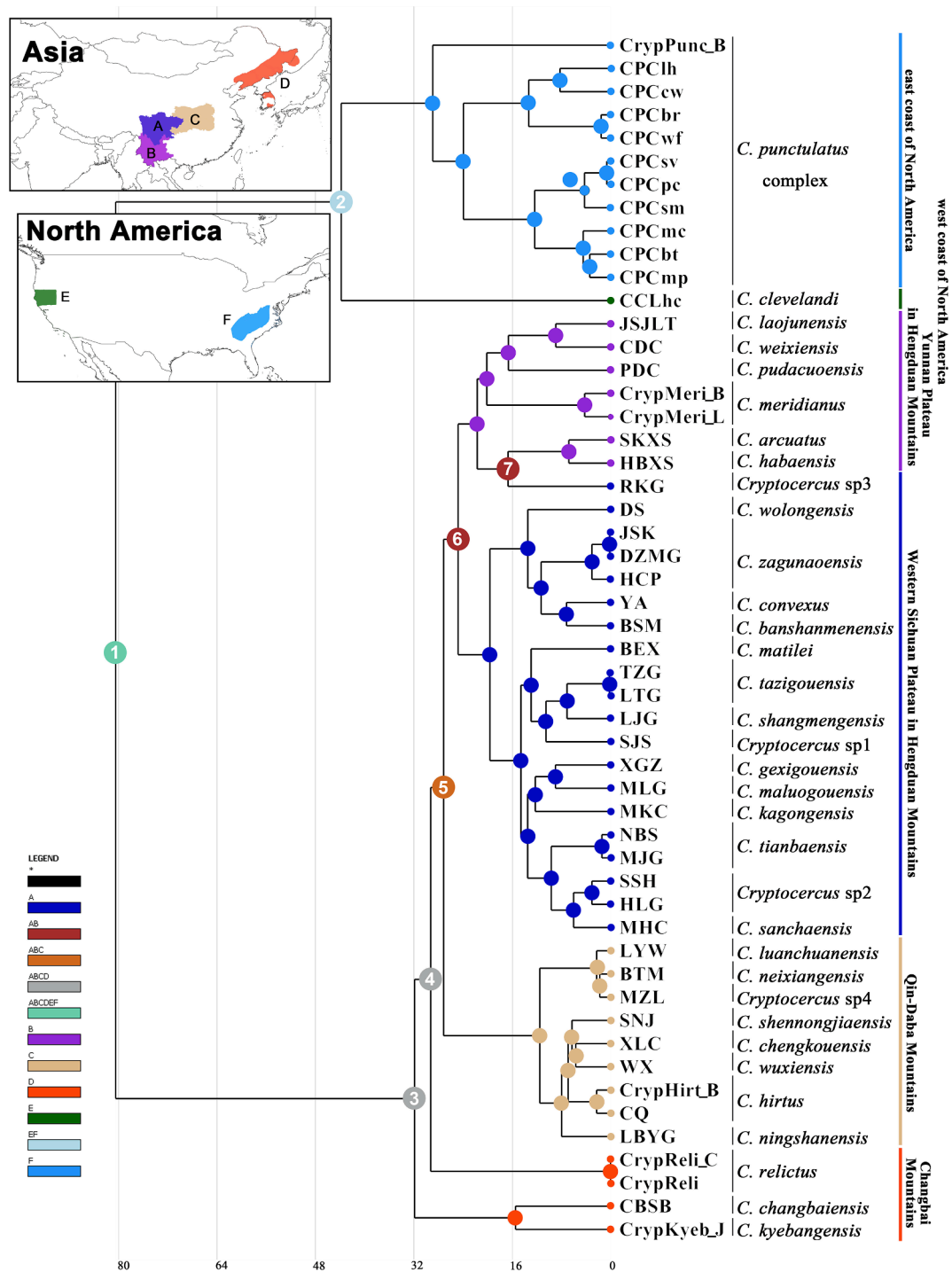

Fig. 6. Reconstruction of ancestal distribution areas using S-DIVA in RASP. We recognised six major biogeographic areas as follows: (A) Western Sichuan Plateau in Hengduan Mountains; (B) Yunnan Plateau in Hengduan Mountains; (C) Qin-Daba Mountains; (D) Changbai Mountains including eastern Russia and South Korea; (E) west coast of North America and (F) east coast of North America. Numbers 3 and 7 at nodes indicate two proposed dispersal events, and others five vicariance events.

Cryptocercus from the Hengduan Mountains and Qin-Daba Mountains was dated at 27.2 Ma (95% CI: 21.9–33.5 Ma). The clade comprising species from the Yunnan Plateau was estimated to have diverged from the species from the Western Sichuan Plateau 24.8 Ma (95% CI: 20.1–30.7 Ma). Most species-level diversifications of *Cryptocercus* occurred during the Miocene.

We reconstructed the *Cryptocercus* ancestral ranges using statistical dispersal-vicariance analysis (S-DIVA) in RASP (Fig. 6). Ancestral *Cryptocercus* were inferred to have been widely distributed in eastern Asia and northern America. We inferred two dispersal events and six vicariance events for *Cryptocercus* (Fig. 6: nodes 1–8) with high credibility scores (1.0). The initial vicariance event (Fig. 6: node 1) occurred between American and Asian lineages at 80.5 Ma, which was followed by one vicariance event within American lineage, and two dispersal plus four vicariance events within the Asian lineage. The vicariance event (Fig. 6: node 2) between *C. clevelandi* from the west coast of USA and the *C. punctulatus* complex from the east coast of USA was inferred to have occurred 43.8 Ma (95% CI: 32.0–57.5 Ma).

Dispersal was inferred to have occurred in the ancestral *Cryptocercus* from northeastern Asia around 25.8–39.5 Ma (Fig. 6: node 3). Subsequently, three vicariance events occurred between *C. relictus* from northeastern China and the remaining *Cryptocercus* species (Fig. 6: node 4, 29.3 Ma), *Cryptocercus* species between Hengduan Mountains and Qin-Daba Mountains (Fig. 6: node 5, 27.2 Ma), and species between Yunnan Plateau and Western Sichuan Plateau (Fig. 6: node 6, 24.8 Ma), respectively. Ultimately, one dispersal (Fig. 6: node 7, 21.7 Ma) and one vicariance (Fig. 6: node 8, 16.7 Ma) event each were inferred from the Yunnan Plateau lineage.

4. Discussion

4.1. Mitochondrial genomic rearrangements in Cryptocercus

Four types of gene rearrangements within the tRNA gene cluster (mainly *trnA-trnR-trnN- trnS1-trnE-trnF*, the underlined gene is encoded by the minority strand) were found in eight *Cryptocercus* species from Qin-Daba Mountains (Fig. 2). Our finding (Fig. 3), as well as that of Li et al. (2017), showed that rearranged genes are often located between ND3 and ND5, and are likely caused by TDRL mechanisms (Liu et al., 2017a, 2017b; Song et al., 2019). Most insects have conserved mt genome arrangements, and rearrangements generally involve a few tRNA genes, with some exceptions, such as the mt genome of a wallaby louse in which all tRNA genes and nine protein-coding genes have been rearranged (Shao et al., 2001). Our results show that mt gene arrangements are variable among closely related lineages. Three closely related species, *C. luanchuanensis*, *C. neixiangensis* and *C.* sp1 also showed different rearrangement types and rate of change of the tRNA genes.

The tRNA gene rearrangements inferred in our study occurred in species from the Qin-Daba Mountains, but not in species from the Hengduan Mountains, where a gene rearrangement event in *C. meridianus* was previously reported (Li et al., 2017). In terms of terrain, the Hengduan Mountains are more complex than the Qin-Daba Mountains, having more fragmented habitats (Che et al., 2020).

4.2. Implications for the phylogeny of North American Cryptocercus and resolution of relationships among taxa from the Hengduan Mountains

Our results support the monophyly of *Cryptocercus* and termites, and the sister group relationship between Asian and North American *Cryptocercus*, in line with a recent mitochondrial genome phylogeny (Bourguignon et al., 2018). In the North American clade, our results almost concur with the results of Kinjo et al. (2018) based on *Blattabacterium* genomes. The phylograms (Fig. 4, S1-S3) based on different datasets (RNAPCG12 or RNAPCG12tRNA) using Bayesian inference and maximum-likelihood recovered the monophyly of *C. clevelandi* and the *C. punctulatus* complex (Kinjo et al., 2018). Relationships among

members of the *C. punctulatus* complex were partly inconsistent with the result of Che et al. (2016), which might be the result of using different types of data and different taxon sampling.

Recent phylogenetic studies (Bai et al., 2018; Che et al., 2016, 2020; Wang et al., 2019) have improved our knowledge of the phylogeny of Asian *Cryptocercus* species, including species and chromosome number diversity and their geographic distributions on the Western Sichuan Plateau. We confirmed the monophyly of the *Cryptocercus* group from the Hengduan Mountains based on various datasets (RNAPCG12 or RNAPCG12tRNA), in contrast to the results of Che et al. (2020), who found that the group was paraphyletic with respect to taxa from the Qin-Daba Mountains. Our phylogenetic results show that the clade *C. changbaiensis* + *C. kyebangensis* is the earliest branching lineage in the Asian lineage, leading to the paraphyly of *Cryptocercus* from the Changbai Mountains (which include areas of northeastern China, Korea, and eastern Russia) with respect to more southern taxa. This result is inconsistent with the monophyly of this group recovered in previous studies (Che et al., 2020; 2016). *C. changbaiensis* was confirmed to be the sister group of *C. kyebangesis*, not *C. relictus*, which is consistent with the result of Che et al. (2020). According to the field investigations of Che et al. (2020), *C. changbaiensis* and *C. relictus* were widely distributed around the Changbai Mountains. Nevertheless, *C. relictus* shares a closer relationship with other *Cryptocercus* groups from the Qin-Daba Mountains and Hengduan Mountains in our analysis. Further study of southwestern Korean *Cryptocercus* from Jiri-san (Park et al., 2004) is therefore warranted.

4.3. The impact of vicariance and dispersal events on global Cryptocercus distributions

Our analyses with seven fossil calibrations based on mitochondrial genomes date the origins of stem-lineage *Cryptocercus c*. 140.5 Ma with 95% CIs (130.3–157.9 Ma), and the split of North American and Asian *Cryptocercus* 80.5 Ma with 95% CIs (60.0–104.7 Ma). Our chronograms have smaller 95% CIs compared with those of previous studies (Che et al., 2016, 2020). The 95% CIs in these previous studies overlap substantially with those inferred here, despite the fact that different data set and fossil calibrations were used. Our results indicate that extant *Cryptocercus* species have evolved over periods of 80.5 My.

Two dispersal and five vicariance events were inferred using statistical dispersal-vicariance analysis (S-DIVA) in RASP and the known distributions of *Cryptocercus* species sampled in this study to reconstruct *Cryptocercus* ancestral ranges. Our results are consistent with the hypothesis that, from the Lower Cretaceous to Upper Jurassic, the ancestor of extant *Cryptocercus* inhabited in the vast forest of the Northern Hemisphere, and that the separation of Asia and North America had important impacts on the modern distribution of *Cryptocercus*. Geological records suggest that the Bering land bridge connected northeastern Asia and north-western North America for much of the time since the Cretaceous (Marincovich and Gladenkov, 1999) which indicates that gene flow between populations of an ancestral *Cryptocercus* species present in both Asia and north-western North America could occur during that time. Although the Bering land bridge remained a potential dispersal corridor until the Pliocene (Gladenkov et al., 2002) (when a continuous belt of boreotropical forests present since the early Paleocene (65 Ma) extended over the entire Northern Hemisphere), the environment of the area across the Bering land bridge was probably suitable for warm-adapted taxa including reptiles and arthropods (Jiang et al., 2019), but inhospitable for *Cryptocercus*. *Cryptocercus* prefers cold and high humidity environments (Maekawa and Nalepa, 2011; Bai et al., 2018; Che et al., 2016, 2020). This may have led to migration southwards by ancestral *Cryptocercus* species, leading to the formation of the Asian and North American lineages. This also coincides with the divergence time of North American and Asian *Cryptocercus* 80.5 Ma (95% CI 60.0–104.7 Ma).

From the early Cretaceous, the North American Inland Sea separated

west and east North America (King, 1958) but receded southwards to the Gulf of Mexico at the end of the Cretaceous. Thus, the ancestors of the North American *Cryptocercus* clade are unlikely to have diverged into western and eastern lineages as a result of this event. During the Paleogene (65–34 Ma), rising mountains over much of north-western North America and the consequent formation of large river systems (Torsvik and Cocks, 2017) led to a natural barrier that hindered the spread of organisms. The second vicariance event 43.8 Ma (95% CI 32.0–57.5 Ma) between western and eastern North American lineages (*C. clevelandi* and *C. punctulatus* complex) is generally consistent with this timeframe.

From the Palaeocene to the Eocene, a broad arid vegetation zone covered all of China, except for northeastern China (Sun, 1979), which was covered by a temperate-subtropical humid vegetation zone (Sun and Wang, 2005). We speculate that the common ancestor of Asian *Cryptocercus* lived in the area encompassing northern China, Far East Russia and South Korea. During the Oligocene, the arid zone in China became narrower in the east, which resulted in subtropical arid and semiarid vegetation emerging in central China, and tropical and subtropical humid vegetation emerging in southern China (Sun and Wang, 2005). This would have allowed the movement of *Cryptocercus* into the Qin-Daba and Hengduan Mountains. In contrast to Che et al. (2020), we inferred a dispersal event (Fig. 6: node 3) to southern areas from northeastern China, Far East Russia and South Korea around 25.8–39.5 Ma. From the early Palaeocene to Eocene, although the terrain of northeastern China was much more elevated than other regions in China, it is thought to have been a large plateau (Ge and Ma, 2007). The wide distribution of *C. changbaiensis* and *C. relictus* around the Changbai Mountains (Che et al., 2020) supports this hypothesis. The dispersal of *Cryptocercus* appears to be governed by the succession of host plants, and can occur over long distances. From the late Eocene to Oligocene, the ancient Changbai Mountains, Zhang Guangcailing and the Korean Peninsula began to uplift (Ge and Ma, 2007). The formation of four volcanoes in the Changbai Mountains (Wan, 2012) is thought to have blocked contact through the plain, which could explain the split occurring between *C. changbaiensis* + *C. kyebangensis* and the ancestor of other Asian species 31.9 Ma (95% CI: 25.8–39.5 Ma), and the distribution patterns of *Cryptocercus* in Northeast Asia. The uplift of the Qinghai-Tibetan Plateau around 30 Ma, to no more than 2000 m (Zhang et al., 2009), played an important role in the vicariance event (Fig. 6: node 4, 29.3 Ma) between *C. relictus* from northeastern China and other species in central and southwestern China. Subsequently, as the Qinghai-Tibetan Plateau continued to rise, more fragmented habitats formed, possibly leading to two vicariance events occurring between the lineages in the Hengduan and Qin-Daba Mountains (Fig. 6: node 5, 27.2 Ma), and between Yunnan and Western Sichuan Plateaus (Fig. 6: node 6, 24.8 Ma). The geographical distribution of *C. arcuatus*, *C. habaensis* and *Cryptocercus* sp3 is very close, and their common ancestor (Fig. 6: node 7, 21.7 Ma) could have easily dispersed across natural barriers to the Western Sichuan Plateau. Following this, they became isolated from each other at 16.7 Ma (Fig. 6: node 8).

The last five divergences suggest ancient vicariance caused by the uplift of mountains, including one divergence event in North America, and four divergence events in Asia. Compared with Che et al. (2020), two dispersal and two more vicariance events were inferred in our study. The inconsistencies between them may be the result of using different taxon sampling and different types of data. Overall, the multiple hypotheses for vicariant divergence proposed above are somewhat preliminary, but we believe that our results point to an important role for vicariance in determining the global distributions of *Cryptocercus*.

5. Conclusions

Our study, based on mitochondrial genome and nuclear gene data, has led to improvements in our understanding of the phylogenetic relationships among *Cryptocercus* species worldwide. We found strong support for the monophyly of taxa from: 1) North America, 2) Asia; 3) the Qin-Daba Mountains; and 4) the Hengduan Mountains. The Western Sichuan Plateau lineage and Yunnan Plateau lineage were also found to be paraphyletic owing to one *Cryptocercus* species from Rekugou of the Western Sichuan Plateau. We were not able to resolve the relationships within *C. punctulatus* complex, however, additional sampling will help to improve our understanding of how *Cryptocercus* evolved in this area. Our statistical dispersal-vicariance analysis provided strong support for both vicariance and dispersal in determining the global distribution of *Cryptocercus*. Plate tectonics, the succession of vegetation, and the uplift of mountains appear to have affected the distribution of *Cryptocercus* through vicariance events, whereas dispersal events have shaped the distribution pattern of *Cryptocercus* in Northeastern Asia and the Hengduan Mountains. These findings provide a framework to better understand the evolution of these wingless insects.

Declaration of Competing Interest

Acknowledgments

Appendix A. Supplementary material

Supplementary data to this article can be found online at https://doi.org/10.1016/j.ympev.2021.107318.

References

Andújar, C., Gómez-Zurita, J., Rasplus, J.-Y., Serrano, J., 2012. Molecular systematics and evolution of the subgenus *Mesocarabus* Thomson, 1875 (Coleoptera: Carabidae: Carabus), based on mitochondrial and nuclear DNA. Zool. J. Linn. Soc.-Lond. 166, 787–804. https://doi.org/10.1111/j.1096-3642.2012.00866.x.

Bai, Q.K., Wang, L.L., Wang, Z.Q., Lo, N., Che, Y.L., 2018. Exploring the diversity of Asian *Cryptocercus* (Blattodea: Cryptocercidae): species delimitation based on chromosome numbers, morphology and molecular analysis. Invertebr. Syst. 32, 69–91. https://doi.org/10.1071/IS17003.

Barber-James, H.M., Gattolliat, J.-L., Sartori, M., Hubbard, M.D., 2008. Global diversity of mayflies (Ephemeroptera, Insecta) in freshwater. Hydrobiologia 595, 339–350. https://doi.org/10.1007/s10750-007-9028-y.

Beccaloni, G.W., 2014. Cockroach Species File Online. Version 5.0/5.0. http://cockroach.speciesfile.org/. (accessed 23 December 2020).

Bell, W.J., Roth, L.M., Nalepa, C.A., 2007. Cockroaches: ecology, behavior, and natural history. The Johns Hopkins University Press, Baltimore.

Bernt, M., Donath, A., Jühling, F., Externbrink, F., Florentz, C., Fritzsch, G., Pütz, J., Middendorf, M., Stadler, P.F., 2013. MITOS: Improved de novo metazoan mitochondrial genome annotation. Mol. Phylogenet. Evol. 69, 313–319. https://doi.org/10.1016/j.ympev.2012.08.023.

Bourguignon, T., Lo, N., Roisin, Y., Šobotník, J., Sillam-Dussès, D., Evans, T.A., 2016. Oceanic dispersal, vicariance and human introduction shaped the modern distribution of the termites Reticulitermes, Heterotermes and Coptotermes. Proc. R. Soc. B. 283, 20160179. https://doi.org/10.1098/rspb.2016.0179.

Bourguignon, T., Lo, N., Šobotník, J., Ho, S.Y.W., Iqbal, N., Coissac, E., Lee, M., Jendryka, M.M., David, S.-D., Křížková, B., Roisin, Y., Evans, T.A., 2017. Mitochondrial Phylogenomics Resolves the Global Spread of Higher Termites, Ecosystem Engineers of the Tropics. Mol. Biol. Evol. 34, 589–597. https://doi.org/10.1093/molbev/msw253.

Bourguignon, T., Tang, Q., Ho, S.Y.W., Juna, F., Wang, Z.Q., Arab, D.A., Cameron, S.L., Walker, J., Rentz, D., Evans, T.A., Lo, N., 2018. Transoceanic Dispersal and Plate

Tectonics Shaped Global Cockroach Distributions: Evidence from Mitochondrial Phylogenomics. Mol. Biol. Evol. 35, 970–983. https://doi.org/10.1093/molbev/msy013.

Burnside, C.A., Smith, P.T., Kambhampati, S., 1999. Three new species of the wood roach, *Cryptocercus* (Blattodea: Cryptocercidae), from the eastern United States. J. Kansas. Entomol. Soc. 72, 361–378.

Cameron, S.L., 2014. Insect Mitochondrial Genomics: Implications for Evolution and Phylogeny. Annu. Rev. Entomol. 59, 95–117. https://doi.org/10.1146/annurev-ento- 011613-162007.

Castresana, J., 2000. Selection of Conserved Blocks from Multiple Alignments for Their Use in Phylogenetic Analysi. Mol. Biol. Evol. 17, 540-552. https://doi.org/ 10.1093/oxfordjournals.molbev.a026334.

Che, Y., Bai, Q., Deng, W., Liao, S., He, J., Ho, S.Y.W., Wang, Z., 2020. Uplift-driven diversification revealed by the historical biogeography of the cockroach *Cryptocercus* Scudder (Blattodea: Cryptocercidae) in eastern Asia. Syst. Entomol. 45, 60–72. https://doi.org/10.1111/syen.v45.110.1111/syen.12379.

Che, Y.L., Wang, D., Shi, Y., Du, X.H., Zhao, Y.Q., Lo, N., Wang, Z.Q., 2016. A global molecular phylogeny and timescale of evolution for *Cryptocercus* woodroaches. Mol. Phylogenet. Evol. 98, 201–209. https://doi.org/10.1016/j.ympev.2016.02.005.

Crampton-Platt, A., Yu, D.W., Zhou, X., Vogler, A.P., 2016. Mitochondrial metagenomics: letting the genes out of the bottle. GigaScience 5, 15. https://doi.org/10.1186/s13742-016-0120-y.

Cui, Y., Béthoux, O., Kondratieff, B., Liu, Y., Ren, D., 2015. Sinosharaperla zhaoi (Insecta: Plecoptera; Early Cretaceous), a Gondwanian element in the northern hemisphere, or just a misplaced species? J. Syst. Paleontol. 13, 883–889. https://doi.org/10.1080/14772019.2014.960903.

Drummond, A.J., Ho, S.Y.W., Phillips, M.J., Rambaut, A., 2006. Relaxed phylogenetics and dating with confidence. PloS Biol. 4, 699–710. https://doi.org/10.1371/journal.pbio.0040088.

Drummond, A.J., Suchard, M.A., Xie, D., Rambaut, A., 2012. Bayesian phylogenetics with BEAUti and the BEAST 1.7. Mol. Biol. Evol. 29, 1969–1973. https://doi.org/10.1093/molbev/mss075.

Du, Z., Hasegawa, H., Cooley, J.R., Simon, C., Jin, Y., Cai, W., Sota, T., Li, H., 2019. Mitochondrial genomics reveals shared phylogeographic patterns and demographic history among three periodical cicada species groups. Mol. Biol. Evol. 36, 1187–1200. https://doi.org/10.1093/molbev/msz051.

Ge, X.H., Ma, W.P., 2007. Mesozoic-Cenozoic tectonic framework of southern Northeast Asia. Geol. China 34, 212–228.

Gladenkov, A.Y., Oleinik, A.E., Marincovich, L., Barinov, K.B., 2002. A refined age for the earliest opening of Bering Strait. Palaeogeogr. Palaeoclimatol. Palaeoecol. 183, 321–328. https://doi.org/10.1016/S0031-0182(02)00249-3.

Ho, S.Y.W., Phillips, M.J., 2009. Accounting for calibration uncertainty in phylogenetic estimation of evolutionary divergence times. Syst. Biol. 58, 367–380. https://doi.org/10.1093/sysbio/syp035.

Jarzembowski, E.A., 1981. An early Cretaceous termite from southern England (Isoptera: Hodotermitidae). Syst. Entomol. 6, 91–96.

Jiang, D., Sebastian, K., Zhang, Y., Hillis, D.M., Li, J., 2019. Asymmetric Biotic Interchange across the Bering Land Bridge between Eurasia and North America. Natl. Sci. Rev. 6, 739–745. https://doi.org/10.1093/nsr/nwz035.

Jiang, P., Li, H., Song, F., Cai, Y., Wang, J., Liu, J., Cai, W., 2016. Duplication and remolding of tRNA genes in the mitochondrial genome of Reduvius tenebrosus (Hemiptera: Reduviidae). Int. J. Mol. Sci. 17, 951. https://doi.org/10.3390/ijms17060951.

King, P.B., 1958. Evolution of modern surface features of western North America. In: Hubbs, C.L. (Ed.), Zoogeography. The American Association for the Advancement of Science, Washington, DC.

Kinjo, Y., Bourguignon, T., Tong, K.J., Kuwahara, H., Lim, S.J., Yoon, K.B., Shigenobu, S., Park, Y.C., Nalepa, C.A., Hongoh, Y., Ohkuma, M., Lo, N., Tokuda, G., 2018. Parallel and Gradual Genome Erosion in the Blattabacterium Endosymbionts of Mastotermes darwiniensis and Cryptocercus Wood Roaches. Genome. Biol. Evol. 10, 1622–1630. https://doi.org/10.1093/gbe/evy110.

Krishna, K., Grimaldi, D., 2009. Diverse Rhinotermitidae and Termitidae (Isoptera) in Dominican amber. Am. Mus. Novit. 80, 1–48.

Krishna, K., Grimaldi, D., 2003. The first Cretaceous Rhinotermitidae (Isoptera): a new species, genus, and subfamily in Burmese amber. Am. Mus. Novit. 3390, 1–10. https://doi.org/10.1206/0003-0082(2003)3902.0.CO;2.

Krosch, M., Cranston, P.S., 2013. Not drowning, (hand)waving? Molecular phylogenetics, biogeography and evolutionary tempo of the 'Gondwanan' midge *Stictocladius* Edwards (Diptera: Chironomidae). Mol. Phylogenet. Evol. 68, 595–603. https://doi.org/10.1016/j.ympev.2013.04.006.

Lanfear, R., Calcott, B., Ho, S.Y.W., Guindon, S., 2012. PartitionFinder: combined selection of partitioning schemes and substitution models for phylogenetic analyses. Mol. Biol. Evol. 29, 1695–1701. https://doi.org/10.1093/molbev/mss020.

Li, W., Wang, Z., Che, Y., 2017. The Complete Mitogenome of the Wood-Feeding Cockroach *Cryptocercus meridianus* (Blattodea: Cryptocercidae) and Its Phylogenetic Relationship among Cockroach Families. Int. J. Mol. Sci. 18, 2397. https://doi.org/10.3390/ijms18112397.

Liu, X., Li, H., Cai, Y., Song, F., Wilson, J.-J., Cai, W.Z., 2017a. Conserved gene arrangement in the mitochondrial genomes of barklouse families Stenopsocidae and Psocidae. Front. Agr. Sci. Eng. 4, 358–365. https://doi.org/10.15302/J-FASE-2017158.

Liu, H., Li, H., Song, F., Gu, W., Feng, J., Cai, W., Shao, R., 2017b. Novel insights into mitochondrial gene rearrangement in thrips (Insecta: Thysanoptera) from the grass thrips, Anaphothrips obscurus. Sci. Rep. 7, 4284. https://doi.org/10.1038/s41598-017-04617-5.

Liu, Y., Li, H., Song, F., Zhao, Y., Wilson, J.J., Cai, W.Z., 2019. Higher-level phylogeny and evolutionary history of Pentatomomorpha (Hemiptera: Heteroptera) inferred from mitochondrial genome sequences. Syst. Entomol. 44, 810–819. https://doi.org/10.1111/syen.12357.

Lohse, M., Drechsel, O., Kahlau, S., Bock, R., 2013. OrganellarGenomeDRAW–a suite of tools for generating physical maps of plastid and mitochondrial genomes and visualizing expression data sets. Nucleic. Acids. Res. 41, 575–581. https://doi.org/10.1093/nar/gkt289.

Lowe, T.M., Eddy, S.R., 1997. tRNAscan-SE: a program for improved detection of transfer RNA genes in genomic sequence. Nucleic. Acids. Res. 25, 955–964. https://doi.org/10.1093/nar/25.5.955.

Maekawa, K., Nalepa, C.A., 2011. Biogeography and phylogeny of wood-feeding cockroaches in the genus *Cryptocercus*. Insects 2, 354–368. https://doi.org/10.3390/insects2030354.

Marincovich, L., Gladenkov, A.Y., 1999. Evidence for an early opening of the Bering Strait. Nature 397, 149–151.

McBride, H.M., Neuspiel, M., Wasiak, S., 2006. Mitochondria: More Than Just a Powerhouse. Curr. Biol. 16, R551–R560. https://doi.org/10.1016/j.cub.2006.06.054.

Misof, B., Liu, S., Meusemann, K., Peters, R.S., Donath, A., Mayer, C., et al., 2014. Phylogenomics resolves the timing and pattern of insect evolution. Science 346, 763–767. https://doi.org/10.1126/science.1257570.

Nalepa, C.A., Byers, G.W., Bandi, C., Sironi, M., 1997. Description of Cryptocercus clevelandi (Dictyoptera: Cryptocercidae) from the northwestern United States, molecular analysis of bacterial symbionts in its fat body, and notes on biology, distribution, and biogeography. Ann. Entomol. Soc. Am. 90, 416–424. https://doi.org/10.1093/aesa/90.4.416.

Nalepa, C.A., Luykx, P., Klass, K.D., Deitz, L.L., 2002. Distribution of karyotypes of the *Cryptocercus punctulatus* species complex (Dictyoptera: Cryptocercidae) in the southern Appalachians: relation to habitat and history. Ann. Entomol. Soc. Am. 95, 276–287. https://doi.org/10.1603/0013-8746(2002)095[0276:DOKOTC]2.0.CO;2.

Park, Y.C., Maekawa, K., Matsumoto, T., Santoni, R., Choe, J.C., 2004. Molecular phylogeny and biogeography of the Korean woodroaches *Cryptocercus* spp. Mol. Phylogenet. Evol. 30, 450–464. https://doi.org/10.1016/S1055-7903(03)00220-3.

Peck, S.B., 1990. Eyeless arthropods of the Galapagos Islands, Ecuador: composition and origin of the cryptozoic fauna of a young, tropical oceanic archipelago. Biotropica 22, 366–381. https://doi.org/10.2307/2388554.

Peck, S.B., Roth, L.M., 1992. Cockroaches of the Galápagos Islands, Ecuador, with descriptions of three new species (Insecta: Blattodea). Can. J. Zool. 70, 2202–2217. https://doi.org/10.1139/z92-297.

Piton, L.E., 1940. Paléontologie du gisement Éocène de Menat. Lechevalier, Paris.

Qiu, L., Liu, Y.C., Wang, Z.Q., Che, Y.L., 2020. The first blattid (Dictyoptera: Blattodea) in Cretaceous amber and the reconsideration of purported Blattidae. Cretaceous Res. 109, 104359 https://doi.org/10.1016/j.cretres.2019.104359.

Rambaut, A., Drummond, A.J., Xie, D., Baele, G., Suchard, M.A., 2018. Posterior summarisation in Bayesian phylogenetics using Tracer 1.7. Syst. Biol. 67, 901–904. https://doi.org/10.1093/sysbio/syy032.

Ronquist, F., Teslenko, M., Mark, v.d.P., Ayres, D.L., Darling, A., Höhna, S., Larget, B., Liu, L., Suchard, M.A., Huelsenbeck, J.P., 2012. MrBayes 3.2: efficient bayesian phylogenetic inference and model choice across a large model space. Syst. Biol. 61, 539–542. https://doi.org/10.1093/sysbio/sys029.

Schlemmermeyer, T., Cancello, E.M., 2000. New fossil termite species: *Dolichorhinotermes dominicanus* from Dominican amber (Isoptera, Rhinotermitidae, Rhinotermitinae). Papéis Avulsos De Zoologia 41, 303–311.

Shao, R., Campbell, N.J.H., Barker, S.C., 2001. Numerous Gene Rearrangements in the Mitochondrial Genome of the Wallaby Louse, *Heterodoxus macropus* (Phthiraptera). Mol. Biol. Evol. 18, 858–865. https://doi.org/10.1093/oxfordjournals.molbev.a003867.

Simon, C., Buckley, T.R., Frati, F., Stewart, J.B., Beckenbach, A.T., 2006. Incorporating Molecular Evolution into Phylogenetic Analysis, and a New Compilation of Conserved Polymerase Chain Reaction Primers for Animal Mitochondrial DNA. Annu. Rev. Ecol. Evol. S. 37, 545–579. https://doi.org/10.1146/annurev.ecolsys.37.091305.110018.

Song, F., Li, H., Liu, G.-H., Wang, W., James, P., Colwell, D.D., Tran, A., Gong, S., Cai, W., Shao, R., 2019. Mitochondrial Genome Fragmentation Unites the Parasitic Lice of Eutherian Mammals. Syst. Biol. 68, 430–440. https://doi.org/10.1093/sysbio/syy062.

Stamatakis, A., Hoover, P., Rougemont, J., 2008. A rapid bootstrap algorithm for the RAxML web servers. Syst. Biol. 57, 758–771. https://doi.org/10.1080/10635150802429642.

Sun, X., 1979. Palynofloristical investigation on the late Cretaceous and Paleocene of China. Acta Phytotaxon. Sin. 17, 8–23.

Sun, X., Wang, P., 2005. How old is the Asian monsoon system?—Palaeobotanical records from China. Palaeogeogr. Palaeoclimatol. Palaeoecol. 222, 181–222. https://doi.org/10.1016/j.palaeo.2005.03.005.

Tamura, K., Stecher, G., Peterson, D., Filipski, A., Kumar, S., 2013. MEGA6: Molecular Evolutionary Genetics Analysis version 6.0. Mol. Biol. Evol. 30, 2725–2729. https://doi.org/10.1093/molbev/mst197.

Torsvik, T.H., Cocks, L.R.M., 2017. Earth History and Palaeogeography. Cambridge University Press, Cambridge.

Toussaint, E.F.A., Gillett, C.P.D.T., 2018. Rekindling Jeannel's Gondwanan vision? Phylogenetics and evolution of Carabinae with a focus on Calosoma caterpillar hunter beetles. Biol. J. Linn. Soc. 123, 191–207. https://doi.org/10.1093/biolinnean/ blx128.

Trewick, S.A., 2001. Molecular evidence for dispersal rather than vicariance as the origin of flightless insect species on the Chatham Islands, New Zealand. J. Biogeogr. 27, 1189–1200. https://doi.org/10.1046/j.1365-2699.2000.00492.x.

Wan, F., 2012. Geological and geomorphological evolution history of Changbai Mountain of Jilin Province. Jilin Geol. 31, 21–23.

Wang, L.L., Liao, S.R., Liu, M.L., Deng, W.B., He, J.J., Wang, Z.Q., Che, Y.L., 2019. Chromosome number diversity in Asian *Cryptocercus* (Blattodea, Cryptocercidae) and implications for karyotype evolution and geographic distribution on the Western Sichuan Plateau. Syst. Biodivers. 17, 594–608. https://doi.org/10.1080/14772000.2019.1659878.

Xia, X., 2018. DAMBE7: New and Improved Tools for Data Analysis in Molecular Biology and Evolution. Mol. Biol. Evol. 35, 1550–1552. https://doi.org/10.1093/ molbev/msy073.

Yu, Y., Harris, A.J., Blair, C., He, X.J., 2015. RASP (Reconstruct Ancestral State in Phylogenies): a tool for historical biogeography. Mol. Phylogenet. Evol. 87, 46–49. https://doi.org/10.1016/j.ympev.2015.03.008.

Zhang, Y.G., Ji, J.F., Balsam, W., Liu, L.W., Chen, J., 2009. Mid-Pliocene Asian monsoon intensification and the onset of Northern Hemisphere glaciation. Geology 37, 599–602. https://doi.org/10.1130/g25670a.1.